

Quantitative Trait Loci that Control Plasma Lipid Levels in an F₂ Intercross between C57BL/6J and DDD.Cg-*A^y* Inbred Mouse Strains

Jun-ichi SUTO^{1)*}

¹⁾Agrogenomics Research Center, National Institute of Agrobiological Sciences, Tsukuba, Ibaraki 305-8634, Japan

(Received 19 September 2011/Accepted 14 November 2011/Published online in J-STAGE 28 November 2011)

ABSTRACT. The objectives of this study were to characterize plasma lipid phenotypes and dissect the genetic basis of plasma lipid levels in an obese DDD.Cg-*A^y* mouse strain. Plasma triglyceride (TG) levels were significantly higher in the DDD.Cg-*A^y* strain than in the B6.Cg-*A^y* strain. In contrast, plasma total-cholesterol (CHO) levels did not substantially differ between the two strains. As a rule, the *A^y* allele significantly increased TG levels, but did not increase CHO levels. Quantitative trait locus (QTL) analyses for plasma TG and CHO levels were performed in two types of F₂ female mice [F₂ *A^y* (F₂ mice carrying the *A^y* allele) and F₂ non-*A^y* (F₂ mice without the *A^y* allele)] produced by crossing C57BL/6J females and DDD.Cg-*A^y* males. Single QTL scan identified one significant QTL for TG levels on chromosome 1, and two significant QTLs for CHO levels on chromosomes 1 and 8. When the marker nearest to the QTL on chromosome 1 was used as covariates, four additional significant QTLs for CHO levels were identified on chromosomes 5, 6, and 17 (two loci). In contrast, consideration of the agouti locus genotype as covariates did not detect additional QTLs. DDD.Cg-*A^y* showed a low CHO level, although it had *Apoa2^b*, which was a CHO-increasing allele at the *Apoa2* locus. This may have been partly due to the presence of multiple QTLs, which were associated with decreased CHO levels, on chromosome 8.

KEY WORDS: cholesterol, mice, plasma lipid levels, quantitative trait locus (QTL), triglyceride.

doi: 10.1292/jvms.11-0430; *J. Vet. Med. Sci.* 74(4): 449–456, 2012

In normal mice, the *agouti* gene is expressed only in the skin [3, 14]. This gene regulates pigmentation by serving as an inverse agonist of the melanocortin 1 receptor [9, 18]. However, in *A^y* mice, the *agouti* gene is ectopically over-expressed because the *A^y* allele is associated with a large deletion and *agouti* gene expression is controlled by an unrelated *Raly* gene promoter [4, 12–14]. Obesity in *A^y* mice is believed to be a consequence of the fact that the *agouti* protein serves as a constitutive antagonist of the melanocortin 4 receptor (MC4R) by mimicking the action of the *agouti*-related protein [7, 16]. MC4R exerts its physiological effects on feeding by mediating signals from melanocortin peptides downstream of leptin signaling [16]. In addition to obesity, *A^y* mice are also characterized by diabetic trend and dyslipidemia.

Female DDD.Cg-*A^y* [a congenic mouse strain for the *A^y* allele at the *agouti* locus on an inbred DDD/Sgn (DDD) strain, hereafter designated DDD-*A^y*] mice exhibited extreme obesity. DDD-*A^y* females were slightly heavier than KK.Cg-*A^y*/Ta (KK-*A^y*) females and significantly heavier than B6.Cg-*A^y*/J (B6-*A^y*) females, i.e., average body weight at 16 weeks was 54.2 g in DDD-*A^y*, 52.2 g in KK-*A^y*, and 38.5 g in B6-*A^y*. Although KK-*A^y* and B6-*A^y* females did not weigh more than 60 g (body weights were measured by 29 weeks), DDD-*A^y* females weighed more than 60 g at 19 weeks and above, and some of them weighed more than 70

g by 22 weeks.

QTL analyses for body weight and obesity (defined by body mass index) was performed in F₂ mice produced by crossing C57BL/6J (B6) females and DDD-*A^y* males [21]. Four significant QTLs for body weight were identified on chromosomes 6, 9, and 17 (two loci), and four significant QTLs for obesity were identified on chromosomes 1, 6, 9, and 17. Because DDD-*A^y* females can serve as mouse models for obesity, it is beneficial to characterize the metabolic aspects of this mouse strain. In this study, plasma lipid phenotypes were characterized in the DDD-*A^y* strain in comparison with the B6-*A^y* strain. Furthermore, QTL analyses were performed for plasma triglyceride (TG) and total-cholesterol (CHO) levels in the same F₂ mice. Because the DDD strain differed genetically from many other inbred mouse strains, novel QTLs for plasma lipid levels were expected to be identified. The possible influence of the *A^y* allele on plasma lipid levels was also investigated.

MATERIALS AND METHODS

Mice: The inbred mouse DDD strain was maintained at the National Institute of Agrobiological Sciences (NIAS, Tsukuba, Ibaraki, Japan). The inbred mouse C57BL/6J Jcl (hereafter B6) strain was purchased from Clea Japan Inc. (Tokyo, Japan). The congenic mouse B6.Cg-*A^y* (hereafter B6-*A^y*) strain was purchased from the Jackson Laboratory (Bar Harbor, ME, U.S.A.). The process of establishing the DDD-*A^y* strain has been described previously [21]. Hereafter, DDD-*A^y* and B6-*A^y* are referred together as “*A^y* mice”. Similarly, their control littermates, DDD and B6, are referred together as “non-*A^y* mice”.

*CORRESPONDENCE TO: SUTO, J., Agrogenomics Research Center, National Institute of Agrobiological Sciences, Tsukuba, Ibaraki 305–8634, Japan.

e-mail: jsuto@affrc.go.jp

DDD-*A^y* males were crossed with B6 females to produce the F₁ generation, and F₁ *A^y* mice were intercrossed with F₁ non-*A^y* mice to produce the F₂ generation. F₂ females were weaned at 4 weeks, and the mice were housed in groups of 4 and 5 during the experimental period.

All mice were maintained in a specific-pathogen-free facility with a regular light cycle (12 hr light and 12 hr dark), and controlled temperature (23 ± 1°C) and relative humidity (50%). Food (CRF-1; Oriental yeast Co., Ltd., Tokyo, Japan) and water were freely available throughout the experimental period. All animal experiments were performed in accordance with the guidelines of the Institutional Animal Care and Use Committee of NIAS.

Experimental measurements: At the age of 16 weeks, body weight of the mice fasted for 4 hr was determined using an electric balance to the nearest 0.01 g. The mice were then killed by an overdose of ether. Using heparin as an anticoagulant, whole blood was drawn from the heart into a plastic tube. Sample tubes were centrifuged at 7,000 r.p.m. for 5 min at 4°C to separate the plasma. The plasma samples were maintained at -80°C until use. Plasma TG and CHO levels were determined enzymatically using commercial clinical kits (Test Wako; Wako Pure Chemical Industries, Osaka, Japan).

Genotyping and QTL analysis: Genomic DNA was isolated from the tails of mice using a commercial DNA extraction kit (Wizard Genomic DNA Purification Kit; Promega, Madison, WI, U.S.A.). Microsatellite sequence length polymorphism was identified after PCR amplification of genomic DNA. The PCR products were separated by 10% polyacrylamide gel electrophoresis and visualized by ethidium bromide staining.

Mice were genotyped for the following marker loci: *D1Mit231*, *D1Mit303*, *D1Mit10*, *D1Mit102*, *D1Mit16*, *Apoa2* (see below), *D1Mit291*, *D2Mit312*, *D2Mit296*, *D2Mit92*, *D3Mit203*, *D3Mit25*, *D3Mit212*, *D4Mit1*, *D4Mit178*, *D4Mit166*, *D4Mit234*, *D5Mit267*, *D5Mit113*, *D5Mit239*, *D5Mit161*, *D5Mit221*, *D6Mit116*, *D6Mit224*, *D6Mit188*, *D6Mit39*, *D6Mit108*, *D6Mit256*, *D6Mit259*, *D7Mit250*, *D7Mit362*, *D8Mit191*, *D8Mit205*, *D8Mit249*, *D8Mit183*, *D9Mit59*, *D9Mit191*, *D9Mit207*, *D9Mit198*, *D9Mit212*, *D10Mit188*, *D10Mit183*, *D10Mit42*, *D10Mit95*, *D11Mit236*, *D11Mit36*, *D11Mit124*, *D11Mit61*, *D12Mit136*, *D12Mit172*, *D12Mit156*, *D12Mit259*, *D12Mit141*, *D12Nds2*, *D13Mit207*, *D13Mit64*, *D13Mit110*, *D13Mit213*, *D13Mit171*, *D14Mit64*, *D14Mit193*, *D14Mit165*, *D15Mit174*, *D15Mit184*, *D15Mit193*, *D16Mit131*, *D16Mit57*, *D16Mit136*, *D16Mit139*, *D16Mit49*, *D17Mit164*, *D17Mit176*, *D17Mit139*, *D17Mit93*, *D17Mit123*, *D18Mit21*, *D18Mit149*, *D18Mit152*, *D18Mit25*, *D19Mit32*, *D19Mit91*, *D19Mit35*, *DXMit166*, *DXMit119*, *DXMit64*, and *DXMit38*.

It is necessary to mention the fact that the chromosome 7 is divided in two parts. As a consequence of introgression of the *Tyr* locus from B6 strain, a mid-part of DDD genome on chromosome 7 has been replaced by a B6 genome in DDD-*A^y* mice. In this study, a region proximal to the B6 region was defined as “chromosome 7.1 (*D7Mit250*)”, while a region distal to the B6 region was defined as “chromosome

7.2 (*D7Mit362*)”.

Normality of the distribution of trait data for each F₂ strain was tested using the Shapiro–Wilk W test (JMP 8.0.2, SAS Institute Japan, Tokyo, Japan). If the trait values did not follow a normal distribution, they were appropriately normalized by using the Box–Cox transformation. Initially, the F₂ *A^y* and F₂ non-*A^y* mice were independently analyzed for a single QTL using the R/qlt [1, 2]. Threshold LOD scores for suggestive ($P < 0.63$) and significant ($P < 0.05$) linkages were determined by performing 1,000 permutations for each trait. For significant QTLs, a 95% confidence interval (CI) was defined by 1.5-LOD fall. After single QTL scans, pairwise evaluations of the potential interaction between loci were performed. At this stage, threshold LOD scores were based strictly on the recommended ones according to “A brief tour of R/qlt” by Broman (<http://www.rqtl.org>). Next, data on F₂ non-*A^y* and F₂ *A^y* mice were combined and analyzed. The calculation of the threshold LOD scores was repeated. The presence or absence of possible statistical interactions between the genotypes at the QTL and *agouti* locus (non-*A^y* and *A^y*) was evaluated by two-way ANOVA.

Apolipoprotein A-II (*Apoa2*) cDNA sequencing and genotyping: Considering *Apoa2* as a convincing candidate gene for QTL for plasma lipid levels on chromosome 1, its cDNA sequence was determined in the DDD strain. mRNA was extracted from the liver using the QuickPrep micro mRNA purification kit (GE Healthcare UK Ltd., U.K.). Reverse transcription was performed using the TaKaRa RNA PCR kit (AMV) ver. 3.0 (Takara Bio Japan Inc., Shiga, Japan). The open reading frame (ORF) was amplified and directly sequenced using the following set of PCR primers: 5'-GCAGCACAGAATCGCAGCACT-3' and 5'-GAGAAACAGGCAGAAGGTAGG-3'.

Apoa2 genotyping was performed by PCR-RFLP method as previously described [24]. Briefly, less than 200 bp PCR fragment at the site from exon 3 to the 3'-untranslated region was amplified by PCR. The PCR product was digested by *XhoI* restriction enzyme (Toyobo Co., Ltd., Osaka, Japan). The *XhoI* could digest the DDD allele but could not the B6 allele.

Lecithin cholesterol acyltransferase (*Lcat*) cDNA sequencing: The cDNA and genomic sequences of *Lcat* were determined in the DDD strain. Using a similar protocol and reagents as for *Apoa2* cDNA sequencing, mRNA was extracted from the brain. The cDNA sequence was amplified and directly sequenced using the following two sets of PCR primers: 5'-GTCAGTAGGCACTGGGCTGT-3' and 5'-GTGGTCCTCCAGGACTGAG-3', and 5'-CTGGCCTGGTAGAGGAGATG-3' and 5'-TTTATAACAGCTAGGTCTTTATTCAGG-3'. In addition, genomic DNA sequencing was also performed. Exon 1 was amplified and sequenced using a primer set of 5'-AGCCAGATCCCAAAGGCTAT-3' and 5'-GGC-CAAGAGAACCTTGACAG-3'. Exons 2–5 were amplified and sequenced using the following two primer sets: 5'-CCTTGAGGAGGGTGTACGAG-3' and 5'-GGTG-GCCAAGAAGAGTCCTT-3', and 5'-TTGGCAAGACCGAATCTGTT-3' and 5'-GTGGTCCTCCAGGACT-

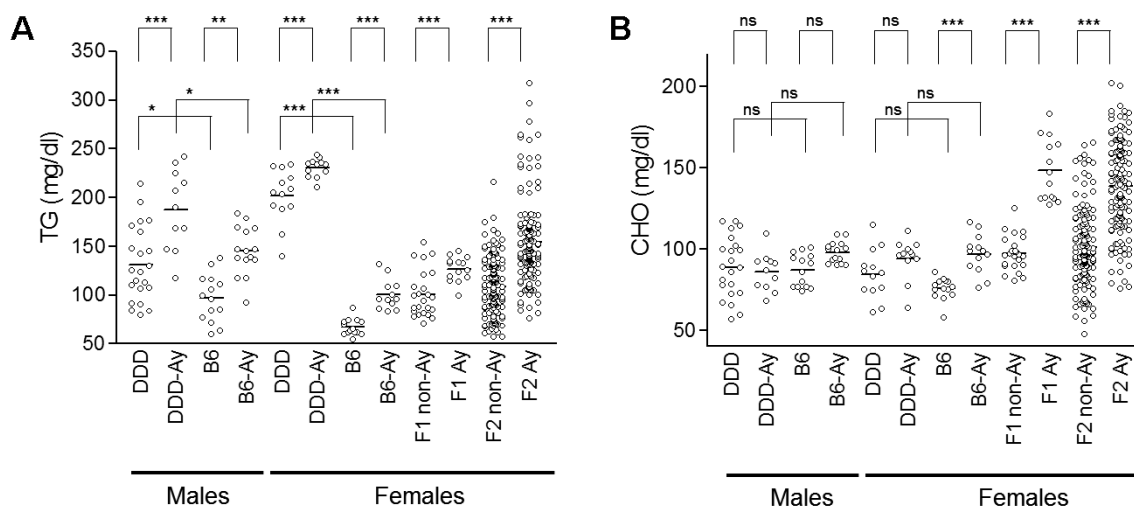


Fig. 1. Plots of TG (A) and CHO (B) in parental, F₁, and F₂ mice. Each point represents the trait value of an individual mouse. The horizontal bar indicates the average levels for each strain. An asterisk denotes significant difference (*: $P < 0.05$, **: $P < 0.01$, ***: $P < 0.001$). ns, not significant.

GAG-3'. Exon 6 was amplified and sequenced using a primer set of 5'-GGTTGTGGCAGAAACAAGGT-3' and 5'-TTAGCAAAGCCCCTGAACC-3'.

Other statistics: Statistical analysis for two groups was performed using Student's or Welch's *t*-test and that for more than two groups was performed using Tukey-Kramer HSD tests by JMP8 (SAS Institute Japan, Tokyo, Japan). $P < 0.05$ was considered to be statistically significant.

RESULTS

Comparison of plasma TG and CHO levels among DDD, DDD-*A^y*, B6, and B6-*A^y* strains: Figure 1 shows scatterplots of plasma lipid [TG (A) and CHO (B)] levels in the DDD males ($n=22$), DDD-*A^y* males ($n=11$), B6 males ($n=14$), B6-*A^y* males ($n=15$), DDD females ($n=13$), DDD-*A^y* females ($n=12$), B6 females ($n=14$), and B6-*A^y* females ($n=13$). Statistical comparisons were separately performed for males and females. Plasma TG levels were significantly higher in the DDD-*A^y* males than in the B6-*A^y* males ($P < 0.02$), whereas plasma CHO levels did not significantly differ between the two strains ($P > 0.1$). Plasma TG levels were significantly higher in the DDD males than in the B6 males ($P < 0.02$), whereas plasma CHO levels did not significantly differ between the two strains ($P > 0.9$). Plasma TG levels were significantly higher in the DDD-*A^y* females than in the B6-*A^y* females ($P < 0.0001$), whereas plasma CHO levels did not significantly differ between the two strains ($P > 0.9$). Plasma TG levels were significantly higher in the DDD females than in the B6 females ($P < 0.0001$), whereas plasma CHO levels did not significantly differ between the DDD and B6 females ($P > 0.2$). When the statistical comparisons were performed between the *A^y* and non-*A^y* mice, plasma TG levels were significantly higher in the *A^y* mice than in the non-*A^y* mice in both sexes. In contrast, plasma CHO

levels did not significantly differ between the *A^y* and non-*A^y* mice, except that B6-*A^y* females had significantly higher CHO levels than did B6 females ($P < 0.0002$).

Plasma lipid levels in B6 × DDD-*A^y* F₁ and F₂ mice: Figure 1 shows scatterplots of plasma lipid [TG (A) and CHO (B)] levels in the F₁ non-*A^y* females ($n=24$), F₁ *A^y* females ($n=14$), F₂ non-*A^y* females ($n=148$), and F₂ *A^y* females ($n=150$). Plasma TG levels were significantly higher in the F₁ *A^y* and F₂ *A^y* mice than in the F₁ non-*A^y* and F₂ non-*A^y* mice, respectively ($P < 0.0002$ and $P < 4.5 \times 10^{-22}$, respectively). Plasma CHO levels were also significantly higher in the F₁ *A^y* and F₂ *A^y* mice than in the F₁ non-*A^y* and F₂ non-*A^y* mice, respectively ($P < 1.5 \times 10^{-12}$ and $P < 3.4 \times 10^{-29}$, respectively). The average TG levels in the F₁ non-*A^y* mice were between those in the DDD and B6 strains. The average TG levels in the F₁ *A^y* mice were between those in the DDD-*A^y* and B6-*A^y* strains. In contrast, the average CHO levels in the F₁ non-*A^y* and F₁ *A^y* mice were higher than those in the parental non-*A^y* and *A^y* strains, respectively. The F₂ mice exhibited a wide spectrum of variations for both traits.

Genome-wide scans for single QTL: First, the F₂ non-*A^y* and F₂ *A^y* mice were analyzed separately. Table 1 shows the results of the single QTL scans. For TG levels, three suggestive QTLs were identified on chromosomes 1, 16, and 18 in the F₂ non-*A^y* mice (Fig. 2A). Three suggestive QTLs were identified on chromosomes 1, 3, and 11 in the F₂ *A^y* mice. For CHO levels, two significant QTLs were identified on chromosomes 1 and 8 in the F₂ non-*A^y* mice (Fig. 2B). I assigned gene symbols *Choldq1* (cholesterol in DDD QTL no. 1) and *Choldq2* to these loci. At *Choldq1*, the DDD allele was associated with increased CHO levels (Fig. 3A). At *Choldq2*, the DDD allele was associated with decreased CHO levels (Fig. 3B). One significant QTL and one suggestive QTL were identified on chromosomes 1 and 11, respectively, in the F₂ *A^y* mice. Because the 95% CI for QTL on

Table 1. QTLs identified in F₂ non-*A^y*, F₂ *A^y*, and combined F₂ (F₂ non-*A^y* plus F₂ *A^y*) mice by single QTL scans

Traits	F ₂ type	Chromosome	Location (cM) ^{a)}	95% CI (cM) ^{b)}	Max LOD ^{c)}	Nearest marker	High allele ^{d)}	Name ^{e)}	
TG	non- <i>A^y</i>	1	86		2.00	<i>D1Mit291</i>	DDD		
		16	37		2.47	<i>D16Mit139</i>	DDD		
		18	59		2.31	<i>D18Mit25</i>	DDD		
	<i>A^y</i>	1	70		2.52	<i>D1Mit16</i>	DDD		
		3	31		2.39	<i>D3Mit25</i>	DDD		
		11	47		2.43	<i>D11Mit36</i>	DDD		
	Combined	1	81	66–89	4.11*	<i>Apoa2</i>	DDD	<i>Trigdql</i>	
		11	37		3.02	<i>D11Mit236</i>	DDD		
	CHO	non- <i>A^y</i>	1	79	76–85	23.10*	<i>Apoa2</i>	DDD	<i>Choldql</i>
			8	50	21–50	3.58*	<i>D8Mit183</i>	B6	
16			22		2.19	<i>D16Mit57</i>	DDD		
<i>A^y</i>		1	79	75–85	13.79*	<i>Apoa2</i>	DDD	<i>Choldql</i>	
		11	56		2.46	<i>D11Mit36</i>	DDD		
Combined		1	79	78–83	35.73*	<i>Apoa2</i>	DDD	<i>Choldql</i>	
		8	49	21–50	4.63*	<i>D8Mit183</i>	B6		<i>Choldq2</i>
		11	60		2.90	<i>D11Mit124</i>	DDD		

a) Location indicates a chromosomal position showing a peak LOD score in cM. b) 95% CI is defined by a 1.5-LOD support interval, and is determined only for significant QTLs. c) Maximum LOD score for QTL. Significant QTLs are indicated by * (suggestive QTLs are presented without asterisk). d) Allele associated with higher trait values. e) Assignment of the QTL name is limited to significant QTLs.

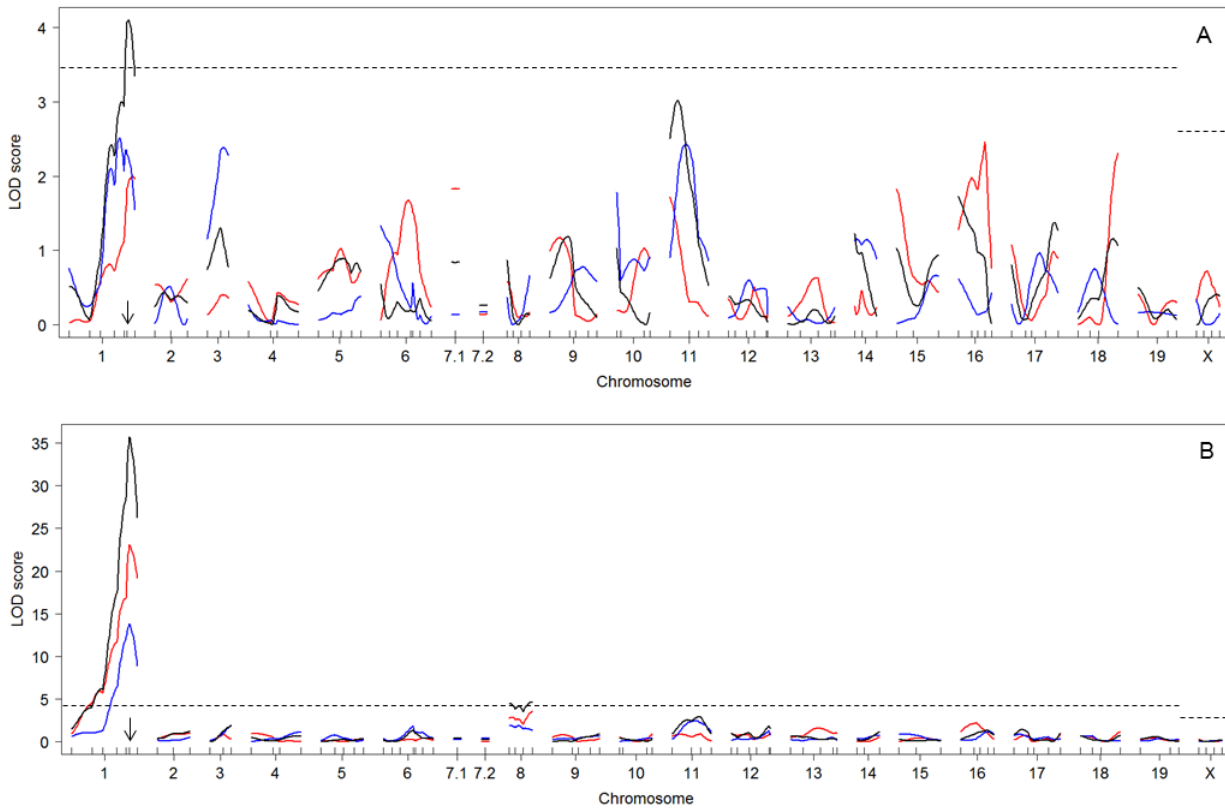


Fig. 2. LOD score plots for plasma TG (A) and CHO levels (B) by single QTL scan. The X-axis represents chromosomes. The Y-axis represents the LOD score. Red lines indicate the LOD scores for F₂ non-*A^y* mice, blue lines indicate the LOD scores for F₂ *A^y* mice, and black solid lines indicate the LOD scores for combined F₂ mice. A horizontal dashed line indicates significant threshold LOD score determined by 1,000 permutations. An arrow indicates the chromosomal position of the *Apoa2*.

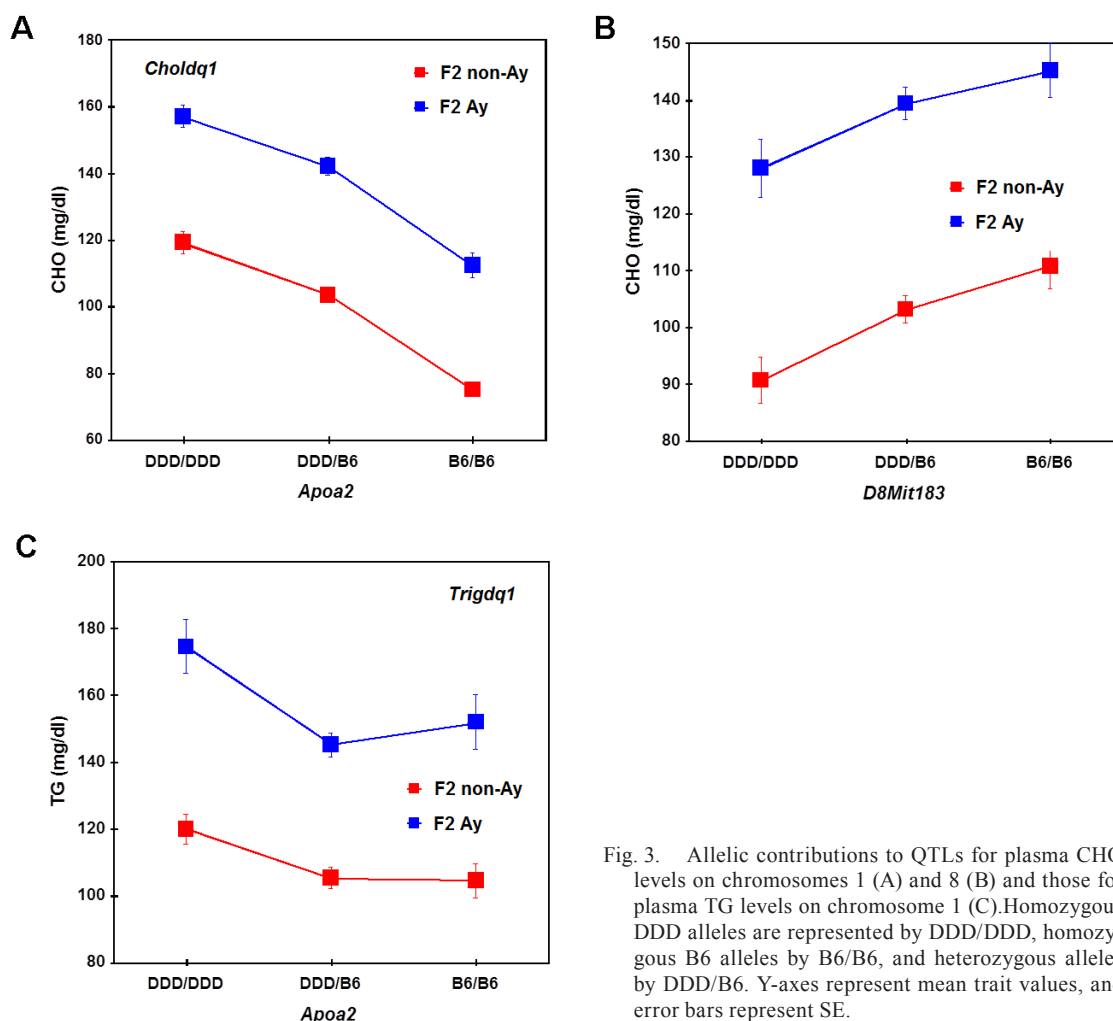


Fig. 3. Allelic contributions to QTLs for plasma CHO levels on chromosomes 1 (A) and 8 (B) and those for plasma TG levels on chromosome 1 (C). Homozygous DDD alleles are represented by DDD/DDD, homozygous B6 alleles by B6/B6, and heterozygous alleles by DDD/B6. Y-axes represent mean trait values, and error bars represent SE.

chromosome 1 overlapped with that for *Choldq1* identified in the F₂ non-*A^y* mice, I assigned the same gene symbol to this locus. The DDD allele was associated with increased CHO levels.

For CHO levels, the LOD scores of *Choldq1* were extremely high in both F₂ non-*A^y* and F₂ *A^y* mice. Therefore, CHO levels were further analyzed by using the marker nearest to *Choldq1* as covariates. When the nearest marker (*D1Mit291* or *D1Mit16*) was included as an additive covariate, the LOD scores on chromosome 1 shrank to near 0 (data not shown), but further significant QTLs were not identified in both F₂ mice (Table 2). When the nearest marker was used as an interactive covariate, one significant QTL was identified on chromosome 17 in F₂ non-*A^y* mice. I assigned gene symbol *Choldq3* to this locus. Since the difference between the LOD score with the nearest marker as an interactive covariate and the LOD score with the nearest marker as an additive covariate concerns the test of the QTL × covariate interaction, this was conducted in F₂ non-*A^y* and F₂ *A^y* mice. One significant QTL was identified on chromosome 5 in F₂ non-*A^y* mice, and two significant QTLs were identified

on chromosomes 6 and 17 in F₂ *A^y* mice (Fig. 4). I assigned gene symbols *Choldq4*, *Choldq5*, and *Choldq6* to these loci, respectively (Table 2). *Choldq3* and *Choldq6* were located on chromosome 17, but they were suggested to be separate loci based on the chromosomal positions.

Next, data on the F₂ non-*A^y* and F₂ *A^y* mice were combined and reanalyzed. For TG levels, one significant QTL and one suggestive QTL were identified on chromosomes 1 and 11, respectively (Table 1, Fig. 2A). I assigned the gene symbol *Trigdq1* (triglyceride in DDD QTL no. 1) to the QTL on chromosome 1. At *Trigdq1*, the DDD allele was associated with increased TG levels (Fig. 3C). For CHO levels, two significant QTLs and one suggestive QTL were identified on chromosomes 1, 8, and 11. When the *agouti* genotype was used as an additive or an interactive covariate in the combined F₂ data set, no significant QTLs were newly identified for both TG and CHO levels (data not shown).

Pairwise genome scans for interacting QTLs: Potential interactions were analyzed pairwise in F₂ non-*A^y* and F₂ *A^y* mice. Threshold LOD scores for significant interactions were based on those recommended in “A brief tour of R/

Table 2. Summary of single QTL scan for plasma CHO levels using the nearest marker to *Choldq1* as covariates

F ₂ type	Chromosome (position, LOD scores, nearest marker, locus name)		
	<i>Choldq1</i> as an additive covariate (LOD _a) ^{a)}	<i>Chldq1</i> as an interactive covariate (LOD _i) ^{b)}	LOD _i (LOD _i -LOD _a) ^{c)}
non- <i>A</i> ^y	None	17 (15 cM, 5.67, <i>D17Mit176</i> , <i>Choldq3</i>)	5 (77 cM, 3.94, <i>D5Mit221</i> , <i>Choldq4</i>)
<i>A</i> ^y	None	None	6 (75 cM, 4.22, <i>D6Mit259</i> , <i>Choldq5</i>) 17 (46 cM, 3.31, <i>D17Mit93</i> , <i>Choldq6</i>)

Peak position (cM) and LOD score is given in parentheses. Only significant QTLs are listed. a) Significant threshold LOD scores are 3.38–3.46 for autosomes and 2.81–2.84 for X chromosome. b) Significant threshold LOD scores are 5.28–5.66 for autosomes and 3.85–4.05 for X chromosome. c) LOD_i is the difference between the LOD score with *Choldq1* as an interactive covariate (LOD_i) and the LOD score with *Choldq1* as an additive covariate (LOD_a). It concerns the test of the QTL × *Choldq1* interaction. Significant threshold LOD scores are 3.28–3.69 for autosomes and 3.64–3.91 for X chromosome.

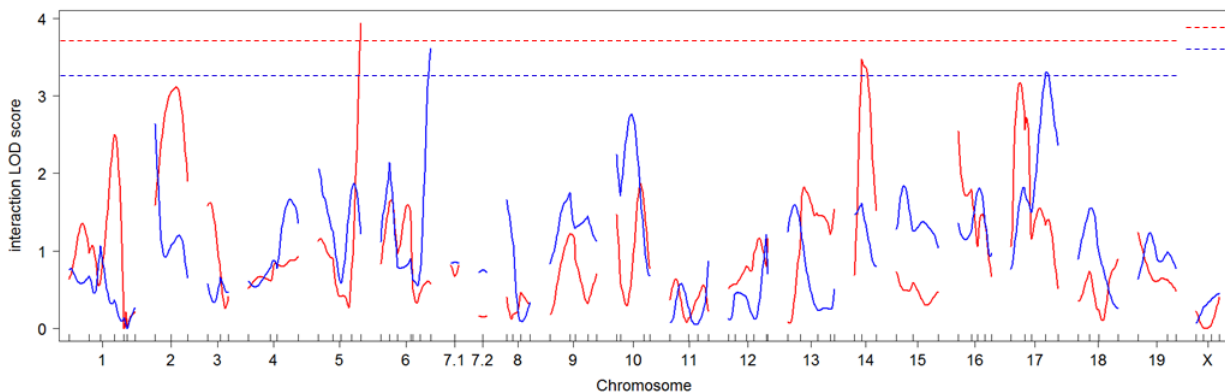


Fig. 4. Interaction LOD score plots for CHO levels. Red lines indicate the LOD score plots for F₂ non-*A*^y mice and blue lines indicate the LOD score plots for F₂ *A*^y mice. Horizontal dashed lines, color-coded by each F₂ type, indicate significant threshold LOD scores determined by 1,000 permutations.

qtl” by Broman (<http://www.rqtl.org>). No significant interactions were identified for TG and CHO levels.

Candidate gene sequencing: Considering *Apoa2* as a plausible candidate gene for *Trigdq1* and *Choldq1* on chromosome 1, its cDNA sequence was determined in DDD and compared with that of B6 (data not shown). The B6 sequence was found to be an *Apoa2^a* allele, while the DDD sequence was revealed to be identical to that of the KK and RR strains, which was an *Apoa2^b* allele [23, 24]. Six nucleotide substitutions were present between the two alleles, and three of them were accompanied by amino acid changes. No nucleotide substitutions were identified for *Lcat* cDNA between the two strains. Of note, *Apoa2* mRNA and *Lcat* mRNA were normally expressed.

DISCUSSION

Plasma TG levels were significantly higher in the DDD and DDD-*A*^y strains than in the B6 and B6-*A*^y strains, respectively. In contrast, plasma CHO levels did not substantially differ between the two strains. Interestingly, the DDD and DDD-*A*^y strains were hypertriglyceridemic without showing a hypercholesterolemic trend. The low CHO level in the DDD strain was an interesting finding considering the fact that this strain had the *Apoa2^b* allele, which is a

CHO-increasing allele among *Apoa2* alleles [23]. In general, mouse strains carrying the *Apoa2^b* allele have higher CHO levels than those carrying other *Apoa2* alleles [27] (see below). The presence of other loci associated with decreased CHO levels in the DDD genome was suggested. *Choldq2* on chromosome 8 was a plausible candidate for such a locus because *Choldq2* exerted its effect in a direction opposite to that of *Choldq1*, i.e., the DDD allele was associated with decreased CHO levels at *Choldq2*. Moreover, the 95% CI of *Choldq2* was quite large and suggested the presence of more than one QTL for CHO levels on chromosome 8. The DDD allele was constantly associated with decreased CHO levels at putative multiple QTLs on this chromosome. As a result, it appeared that QTLs on this chromosome may substantially decrease CHO levels. *Choldq2* contained a candidate gene *Lcat* in its 95% CI. In *Lcat*-deficient mice, CHO levels were significantly decreased, but TG levels were significantly or substantially increased [15, 19]. Although sequence differences were not identified in ORF of *Lcat* cDNA between the DDD and B6 strains, its candidacy cannot be denied. Coincidental QTLs have been reported to a relevant region of chromosome 8. Mehrabian *et al.* [11] identified one QTL for high-density lipoprotein (HDL)-CHO levels at 53.18 cM on chromosome 8 in an F₂ intercross between CAST/Ei and B6. *Lcat*

was located at 53.06 on this chromosome, and they regarded it as a primary candidate gene for the QTL. Although the CAST/Ei strain had a normal level of *Lcat* mRNA, it showed reduced *Lcat* activity. The CAST/Ei allele was associated with decreased HDL-CHO levels. In the *Lcat* ORF, two nucleotide changes were identified between the two strains and both changes were accompanied by amino acid substitution. However, the QTL was a suggestive one, and therefore, only a small fraction of phenotypic variation can be attributed to this QTL. Ishimori *et al.* [8] identified one QTL for HDL-CHO levels (*Hdlq16*) at 44 cM on chromosome 8 in an F₂ intercross between B6 and 129S1/SvImJ strains. At *Hdlq16*, the high HDL-CHO strain 129S1/SvImJ allele was associated with increased HDL-CHO levels. Although this QTL was a suggestive one, they assigned the abovementioned gene symbol because they considered this study to confirm the results of Mehrabian *et al.* [11]. Thus, only a few QTLs for CHO levels have been identified on chromosome 8, and on this point, the DDD strain could be regarded as a valuable resource strain.

For CHO levels, inclusion of the marker nearest to *Choldq1* as covariates allowed identification of additional significant QTLs on chromosomes 5, 6, and 17 (Table 2, Fig. 4). These QTLs were suggested to interact with *Apoa2* gene. Intriguingly, among these QTLs, *Choldq5* was of great interest because *Lipq1* was reported as a coincidental QTL [28]. *Lipq1* was identified in F₂ female population by controlling the effect of the *Apoa2* allele. *Choldq5* may be allelic with *Lipq1*. Even so, we should be cautious of the understanding of this interaction because rigorous pairwise scan did not identify any significant interactions. Inclusion of the agouti genotype as covariates did not give increased power to detect further QTLs, although it has large phenotype effect. In F₂ mice, the *A^y* mice had significantly higher plasma lipid levels than did the non-*A^y* mice (Fig. 1). Probably, the effect of the *A^y* allele might be simple and additive to a single QTL. In fact, the F₂ *A^y* mice had substantially higher lipid levels than the F₂ non-*A^y* mice at all significant QTLs, but the mode of inheritance of QTLs did not significantly differ between the two F₂ types (Fig. 3).

Single QTL scans identified *Trigdq1* and *Choldq1* in the overlapping regions on chromosome 1. A plausible candidate gene for these QTLs was *Apoa2*. To our knowledge, the gene underlying QTLs for CHO levels that has been mapped to a distal region of chromosome 1 is *Apoa2*. Except for rare alleles found in wild-derived strains, three different *Apoa2* alleles are known to be present in laboratory mouse strains. According to Higuchi *et al.* [6], the *Apoa2* allele from the B6 strain is defined as *Apoa2^a* and that from the DDD strain is defined as *Apoa2^b*. A third allele, *Apoa2^c*, is found in A/J and SM/J strains. Of the three alleles, *Apoa2^b* is unique in its ability to increase CHO levels. Indeed, when QTLs for CHO levels are located over the gene for *Apoa2* in F₂ mice produced by a cross between two inbred mouse strains, the presence of a combination of different *Apoa2* alleles between the two strains is indicated. This is exemplified in many studies [10, 11, 17, 23–25]. In these F₂ sets, the *Apoa2^b* is always associated with increased CHO levels.

In contrast, QTLs for CHO levels were not mapped to the *Apoa2* region in the absence of a combination of different *Apoa2* alleles in the cross analyzed [22]. In short, QTLs for CHO levels were identified in the *Apoa2* region only when the cross was *Apoa2^b* × *Apoa2^a* or *Apoa2^b* × *Apoa2^c*. This *Apoa2* effect was considered to be due to C-to-T substitution at nucleotide 182, resulting in Ala-to-Val substitution at amino acid residue 61 [23, 27]. In *Apoa2*-deficient mice, CHO levels were dramatically decreased, but TG levels were not substantially changed [29]. In transgenic mice overexpressing *Apoa2*, TG levels were significantly increased 2–3-fold (CHO levels were also significantly increased) [5]. Thus, it seems possible that the *Apoa2* has role in CHO and TG metabolism. The difference in the LOD score between *Choldq1* (35.73) and *Trigdq1* (4.11) was suggested to be a reflection of the difference in the intensity of the *Apoa2* effect. Similar results were obtained in our previous QTL study for plasma CHO and TG levels in an F₂ intercross between B6 and RR strains [23]. Significant QTLs for CHO and TG levels (*Cq6* and *Tgq3*, respectively) were identified on distal chromosome 1. We considered *Apoa2* was the candidate for these QTLs because the RR strain had the *Apoa2^b* allele. The maximum LOD scores for *Cq6* and *Tgq3* were 16.3 and 4.4, respectively. Stewart *et al.* [20] also identified significant QTLs for plasma CHO and TG levels on distal chromosome 1 in an F₂ intercross between B6 and TALLHO/JngJ strains. Hyperlipidemic TALLYHO/JngJ strain had the *Apoa^b* allele, and they considered the *Apoa2* a candidate gene. The maximum LOD scores of QTLs for CHO and TG levels were 11.83 and 3.67, respectively. In contrast to CHO levels, only four QTLs for TG levels have been mapped to distal chromosome 1 [26]; therefore, further studies are needed to evaluate the candidacy of *Apoa2* as causative genes for plasma lipid QTLs.

In summary, the DDD and DDD-*A^y* strains were hypertriglyceridemic without showing a hypercholesterolemic trend. QTL analyses identified one significant QTL for TG levels and three significant QTLs for CHO levels. Identification of the genes underlying these QTLs will make the DDD and DDD-*A^y* strains more valuable as animal models for metabolic research.

ACKNOWLEDGMENT. This study was supported in part by a grant from Kieikai Research Foundation.

REFERENCES

1. Broman, K. W. and Sen, Š. 2009. A Guide to QTL Mapping with R/qtl, Springer, New York.
2. Broman, K. W., Wu, H., Sen, Š. and Churchill, G. A. 2003. R/qtl: QTL mapping in experimental crosses. *Bioinformatics* **19**: 889–890. [Medline] [CrossRef]
3. Bultman, S. J., Michaud, E. J. and Woychik, R. P. 1992. Molecular characterization of the mouse agouti locus. *Cell* **71**: 1195–1204. [Medline] [CrossRef]
4. Duhl, D. M., Vrieling, H., Miller, K. A., Wolff, G. L. and Barsh, G. S. 1994. Neomorphic agouti mutations in obese yellow mice. *Nat. Genet.* **8**: 59–65. [Medline] [CrossRef]
5. Hedrick, C. C., Castellani, L. W., Warden, C. H., Puppione,

- D. L. and Lusis, A. J. 1993. Influence of mouse apolipoprotein A-II on plasma lipoproteins in transgenic mice. *J. Biol. Chem.* **268**: 20676–20682. [Medline]
6. Higuchi, K., Kitagawa, K., Naiki, H., Hanada, K., Hosokawa, M. and Takeda, T. 1991. Polymorphism of apolipoprotein A-II (apoA-II) among inbred strains of mice. *Biochem. J.* **279**: 427–433. [Medline]
 7. Huszar, D., Lynch, C. A., Fairchild-Huntress, V., Dunmore, J. H., Fang, Q., Berkemeier, L. R., Gu, W., Kesterson, R. A., Boston, B. A., Cone, R. D., Smith, F. J., Campfield, L. A., Burn, P. and Lee, F. 1997. Targeted disruption of the melanocortin-4 receptor results in obesity in mice. *Cell* **88**: 131–141. [Medline] [CrossRef]
 8. Ishimori, N., Li, R., Kelmenson, P. M., Korstanje, R., Walsh, K. A., Churchill, G. A., Forsman-Semb, K. and Paigen, B. 2004. Quantitative trait loci analysis for plasma HDL-cholesterol concentrations and atherosclerosis susceptibility between mouse strains C57BL/6J and 129S1/SvImJ. *Arterioscler. Thromb. Vasc. Biol.* **24**: 161–166. [Medline] [CrossRef]
 9. Lu, D., Willard, D., Patel, I. R., Kadwell, S., Overton, L., Kost, T., Luther, M., Chen, W., Woychik, R. P., Wilkison, W. O. and Cone, R. D. 1994. Agouti protein is an antagonist of the melanocyte-stimulating-hormone receptor. *Nature* **371**: 799–802. [Medline] [CrossRef]
 10. Machleder, D., Ivandic, B., Welch, C., Castellani, L., Reue, K. and Lusis, A. J. 1997. Complex genetic control of HDL levels in mice in response to an atherogenic diet. Coordinate regulation of HDL levels and bile acid metabolism. *J. Clin. Invest.* **99**: 1406–1419. [Medline] [CrossRef]
 11. Mehrabian, M., Castellani, L. W., Wen, P. Z., Wong, J., Rithaporn, T., Hama, S. Y., Hough, G. P., Johnson, D., Albers, J. J., Mottino, G. A., Frank, J. S., Navab, M., Fogelman, A. M. and Lusis, A. J. 2000. Genetic control of HDL levels and composition in an interspecific mouse cross (CAST/Ei × C57BL/6J). *J. Lipid Res.* **41**: 1936–1946. [Medline]
 12. Michaud, E. J., Bultman, S. J., Stubbs, L. J. and Woychik, R. P. 1993. The embryonic lethality of homozygous lethal yellow mice (Ay/Ay) is associated with the disruption of a novel RNA-binding protein. *Genes Dev.* **7**: 1203–1213. [Medline] [CrossRef]
 13. Michaud, E. J., Bultman, S. J., Klebig, M. L., van Vugt, M. J., Stubbs, L. J., Russell, L. B. and Woychik, R. P. 1994. A molecular model for the genetic and phenotypic characteristics of the mouse lethal yellow (Ay) mutation. *Proc. Natl. Acad. Sci. U.S.A.* **91**: 2562–2566. [Medline] [CrossRef]
 14. Miller, M. W., Duhl, D. M., Vrieling, H., Cordes, S. P., Ollmann, M. M., Winkes, B. M. and Barsh, G. S. 1993. Cloning of the mouse agouti gene predicts a secreted protein ubiquitously expressed in mice carrying the lethal yellow mutation. *Genes Dev.* **7**: 454–467. [Medline] [CrossRef]
 15. Ng, D. S., Francone, O. L., Forte, T. M., Zhang, J., Haghpassand, M. and Rubin, E. M. 1997. Disruption of the murine lecithin: cholesterol acyltransferase gene causes impairment of adrenal lipid delivery and up-regulation of scavenger receptor class B type I. *J. Biol. Chem.* **272**: 15777–15781. [Medline] [CrossRef]
 16. Ollmann, M. M., Wilson, B. D., Yang, Y. K., Kerns, J. A., Chen, Y., Gantz, I. and Barsh, G. S. 1997. Antagonism of central melanocortin receptors in vitro and in vivo by agouti-related protein. *Science* **278**: 135–138. [Medline] [CrossRef]
 17. Purcell-Huynh, D. A., Weinreb, A., Castellani, L. W., Mehrabian, M., Doolittle, M. H. and Lusis, A. J. 1995. Genetic factors in lipoprotein metabolism. Analysis of a genetic cross between inbred mouse strains NZB/BINJ and SM/J using a complete linkage map approach. *J. Clin. Invest.* **96**: 1845–1858. [Medline] [CrossRef]
 18. Robbins, L. S., Nadeau, J. H., Johnson, K. R., Kelly, M. A., Rosell-Rehffuss, L., Baack, E., Mountjoy, K. G. and Cone, R. D. 1993. Pigmentation phenotypes of variant extension locus alleles result from point mutations that alter MSH receptor function. *Cell* **72**: 827–834. [CrossRef]
 19. Sakai, N., Vaisman, B. L., Koch, C. A., Hoyt, R. F., Meyu, S. M., Talley, G. D., Paiz, J. A., Brewer, H. B. and Santamarina-Fojo, S. 1997. Targeted disruption of the mouse lecithin: cholesterol acyltransferase (LCAT) gene. *J. Biol. Chem.* **272**: 7506–7510. [Medline] [CrossRef]
 20. Stewart, T. P., Kim, H. Y., Saxton, A. M. and Kim, J. H. 2010. Genetic and genomic analysis of hyperlipidemia, obesity and diabetes using (C57BL/6J × TALLYHO/JngJ) F₂ mice. *BMC Genomics* **11**: 713. [Medline] [CrossRef]
 21. Suto, J. 2011. Quantitative trait loci that control body weight and obesity in an F₂ intercross between C57BL/6J and DDD. Cg-A^g mice. *J. Vet. Med. Sci.* **73**: 907–915. [Medline] [CrossRef]
 22. Suto, J. and Sekikawa, K. 2003. Quantitative trait locus analysis of plasma cholesterol and triglyceride levels in KK × RR F₂ mice. *Biochem. Genet.* **41**: 325–341. [Medline] [CrossRef]
 23. Suto, J., Takahashi, Y. and Sekikawa, K. 2004. Quantitative trait locus analysis of plasma cholesterol and triglyceride levels in C57BL/6J × RR F₂ mice. *Biochem. Genet.* **42**: 347–363. [Medline] [CrossRef]
 24. Suto, J., Matsuura, S., Yamanaka, H. and Sekikawa, K. 1999. Quantitative trait loci that control plasma lipid concentrations in hereditary obese KK and KK-A^g mice. *Biochim. Biophys. Acta* **1453**: 385–395. [Medline]
 25. Wang, J., Kitagawa, K., Kitado, H., Kogishi, K., Matsushita, T., Hosokawa, M. and Higuchi, K. 1997. Regulation of the metabolism of plasma lipoproteins by apolipoprotein A-II. *Biochim. Biophys. Acta* **1345**: 248–258. [Medline]
 26. Wang, X. and Paigen, B. 2005. Genome-wide search for new genes controlling plasma lipid concentrations in mice and humans. *Curr. Opin. Lipidol.* **16**: 127–137. [Medline] [CrossRef]
 27. Wang, X., Korstanje, R., Higgins, D. and Paigen, B. 2004. Haplotype analysis in multiple crosses to identify a QTL gene. *Genome Res.* **14**: 1767–1772. [Medline] [CrossRef]
 28. Welch, C. L., Bretscger, S., Wen, P.Z., Mehrabian, M., Latib, N., Fruchart-Najib, J., Fruchart, J. C., Myrick, C. and Lusis, A. J. 2004. Novel QTLs for HDL levels identified in mice by controlling for *Apoa2* allelic effects: confirmation of a chromosome 6 locus in a congenic strain. *Physiol. Genomics* **17**: 48–59. [Medline] [CrossRef]
 29. Weng, W. and Breslow, J. L. 1996. Dramatically decreased high density lipoprotein cholesterol, increased remnant clearance, and insulin hypersensitivity in apolipoprotein A-II knockout mice suggest a complex role for apolipoprotein A-II in atherosclerosis susceptibility. *Proc. Natl. Acad. Sci. U.S.A.* **93**: 14788–14794. [Medline] [CrossRef]